PHYSICAL REVIEW B **77**, 180507(R) (2008)

First-principles study of superconductivity and Fermi-surface nesting in ultrahard transition metal carbides

Jesse Noffsinger, Feliciano Giustino, Steven G. Louie, and Marvin L. Cohen
Department of Physics, University of California at Berkeley, Berkeley, California 94720, USA
and Materials Sciences Division, Lawrence Berkeley National Laboratory, Berkeley, California 94720, USA
(Received 8 April 2008; published 20 May 2008)

Using a recently developed first-principles approach, we show that the variation in the superconducting behavior of group IVb and Vb transition metal carbides is associated with a significant nesting of the Fermi surfaces in group Vb compounds, while their phonon anomalies and density of states at the Fermi level play a minor role. The superconducting pairing arises from the coupling of metal *d* states to acoustic phonons, and is therefore at variance with the interaction leading to the exceptional mechanical hardness where carbon *p* states play a substantial role. We provide insight into how to optimize the transition temperature by varying the Fermi surface properties through substitutional doping.

DOI: 10.1103/PhysRevB.77.180507 PACS number(s): 74.62.Bf, 74.20.−z, 74.25.Jb, 74.70.−b

The discovery of superconductivity at 39 K in magnesium diboride[1] has generated a renewed interest in phonon-mediated superconductors containing light elements. Within this class of materials, carbon and nitrogen compounds have attracted considerable attention following the synthesis of alkali-metal-doped fullerenes, layered hafnium nitride, metal-intercalated graphite, and boron-doped diamond, which have been reported to superconduct at 33 K,[2] 25 K,[3] 11 K[4], and 4 K,[5], respectively. Among the binary carbon compounds, the carbides of the group IVb, Vb, and VIb transition metals (including WC, TiC, TaC, and HfC) exhibit exceptional mechanical properties, with Young moduli as large as 530 GPa and melting temperatures above 3000 K.[6] The mechanical hardness of transition metal carbides has been suggested to originate from bonding combinations of metal *d* and carbon *p* orbitals, which strongly resist shear strain or shape change.[7,8] If a similar mechanism were active in the superconducting pairing, combined with the large frequencies of the optical phonons (~80 meV), this would result in high superconducting transition temperatures.[9] However, experiments performed on carbides and nitrides of the groups IVb, Vb, and VIb transition metals indicate transition temperatures not exceeding 17 K.[6] It is important to understand why such a mechanism seems ineffective in the superconductivity of the carbides, and whether it can be enhanced by chemical doping in order to optimize the transition temperature.

The carbides of the groups IVb and Vb transition metals exhibit similar structural, electronic, and vibrational properties.[6] These compounds all crystallize in the rock-salt structure with similar lattice parameters. The vibrational spectra display acoustic peaks between 10 and 30 meV and optical peaks at 60–90 meV. Despite these similarities, group Vb transition metal carbides exhibit superconductivity in the range 7–11 K,[10] while the IVb compounds have not been observed to superconduct above 0.1 K.[11] These different superconducting properties have variously been ascribed to Kohn anomalies in the vibrational spectra[13] or nesting effects of the associated Fermi surfaces.[14,15] While those studies provided significant insight into the superconductivity of transition metal carbides, a comprehensive study of the interplay between phonon softening, Fermi surface nesting, and carrier concentration in these materials, along with its effect on the superconducting properties, is not available.

In this work, we investigate the superconductivity in transition metal carbides by focusing on two representative compounds, one for each group: HfC (IVb) and TaC (Vb). Using a recently developed first-principles approach to the electron-phonon interaction based on Wannier functions,[16,17] we show that superconductivity in TaC relates to a nesting of the corresponding Fermi surface with large connecting wave vectors. On the other hand, in HfC the Fermi surface does not exhibit a significant nesting and the associated transition temperature is negligibly small. The microscopic mechanism of the pairing is shown to consist of the coupling of the metal *d* states to acoustic zone-edge vibrations. In view of optimizing the transition temperature, we study the variation of the electron-phonon coupling strength with changes in the chemical potential, as well as the onset of structural phase transitions driven by doping through phonon softening.

Calculations were performed within the local-density approximation [18] to density-functional theory.[19] The lattice-dynamical properties were computed in the harmonic approximation using density functional perturbation theory.[20] Superconductivity was studied within the isotropic approximation to the Migdal–Eliashberg theory.[21] The evaluation of the electron-phonon coupling strength $\lambda_{\mathbf{q}}$ and the Eliashberg function $\alpha^2F(\omega)$ required a very dense sampling of the electron-phonon scattering processes throughout the Brillouin zone.[16] We achieved such a dense sampling by means of our first-principles interpolation scheme[16,17] based on maximally localized Wannier functions.[22] In this work, we considered eight electronic Wannier functions spanning an energy range of ±4 eV from the Fermi level. These correspond to five metal *d* states and three carbon *p* states. We computed the electron-phonon matrix elements starting from an initial Brillouin zone mesh with $6\times6\times6$ points, corresponding to a real-space interaction range of 27 Å between image Wannier functions in neighboring supercells.[16] The fine grid for the Brillouin zone integration consisted of $20\times20\times20$ unique points obtained by randomly translating a uniform mesh.

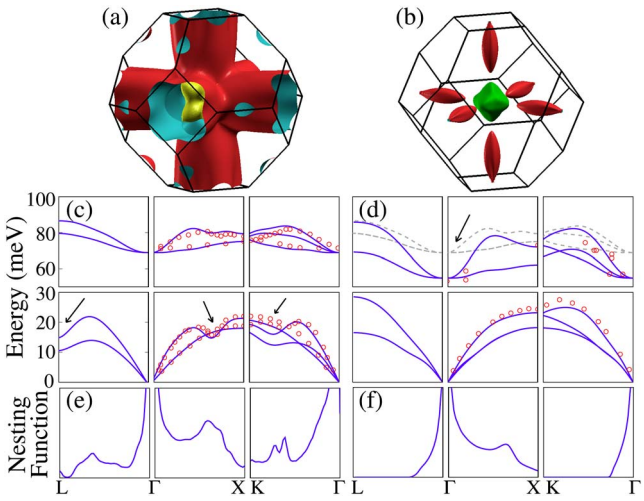

FIG. 1. (Color online) Top: Fermi surfaces of (a) TaC and (b) HfC. Middle: phonon dispersions of (e) TaC and (f) HfC (solid lines), together with the experimental data of Ref. 23 (circles). The dashed lines in (d) correspond to the dispersions of TaC after rescaling the Ta mass to the Hf value. The arrows indicate the wave vectors exhibiting Kohn anomalies. Bottom: Nesting functions of (e) TaC and (f) HfC (arbitrary units).

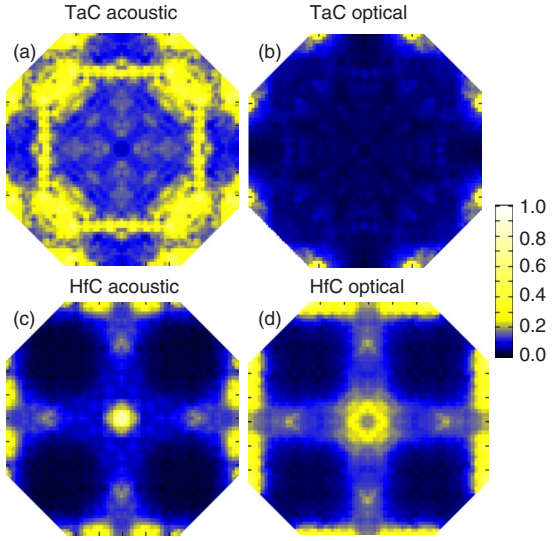

FIG. 2. (Color online) Intensity plot of the electron-phonon coupling strength $\lambda(\mathbf{q})$ in the $\mathbf{q}=(q_x,q_y,0)$ plane of the Brillouin zone. Top: average electron-phonon coupling strength in TaC for acoustic (a) and optical (b) modes. Bottom: average coupling strength in HfC for acoustic (c) and optical (d) modes.

Figure 1 shows the calculated phonon dispersions for TaC and HfC along relevant high-symmetry directions in the Brillouin zone. Our calculations are in good agreement with the dispersions derived from neutron scattering experiments.[23] Pronounced softenings are observed for the acoustic branches of TaC [Fig. 1(c)] at wave vectors corresponding to the L point, to points at 0.7 $\overline{\Gamma X}$, and 0.9 $\overline{\Gamma K}$ in the Brillouin zone. Taken together, these points define a cubic Kohn-anomaly surface in the Brillouin zone,[10] with the corners touching the eight L points and the faces bulging out along the Δ directions. Analogous anomalies can be observed in the vibrational spectra of the other group Vb transition metal carbides NbC and VC.[12,23] Such a Kohn-anomaly surface is not observed in HfC, consistent with the other group IVb compounds ZrC and TiC.[23,24] Nonetheless, close to the zone center the optical phonons of HfC appear significantly softer than what is expected on the basis of a mass scaling argument between HfC and TaC (Fig. 1).

The softening of the acoustic branches in group Vb carbides has been associated with the topology of the corresponding Fermi surface.[14] The Fermi surface of TaC consists of six arms extending from Γ along the Δ directions [Fig. 1(a)], and exhibits important nesting features associated with several wave vectors connecting the parallel faces of the arms. Together, these nesting wave vectors define precisely the Kohn-anomaly surface discussed above. In the case of HfC, the Fermi surface consists of a small spheroid centered at the Γ point and six pockets elongated along the Δ directions. The softening of the zone-center optical phonons of HfC reflects the increased electronic susceptibility for wave vectors corresponding to transitions within the spheroid and within each pocket.

In order to identify the phonons that are relevant to the superconducting pairing, we calculated the electron-phonon coupling strength $\lambda(\mathbf{q})$ [see Eq. (7.23) of Ref. 25] using our Wannier interpolation scheme. For clarity, we consider here the average coupling strength corresponding to the acoustic $[\lambda_{ac}(\mathbf{q})]$ and to the optical $[\lambda_{op}(\mathbf{q})]$ branches (Fig. 2). In the case of TaC, the primary contribution to the acoustic coupling strength arises from wave vectors belonging to the cubic Kohn anomaly surface discussed above. This finding is consistent with the observation that the electron–phonon coupling strength $\lambda(\mathbf{q})$ and the renormalization of the phonon dispersions are both related to the phonon self-energy. The optical modes of TaC appear to offer no significant contribution to the coupling strength. In the case of HfC, both the acoustic and optical branches display significant structure near the zone center, consistent with the softening discussed in relation to Fig. 1(d). In order to quantify the contributions arising from the acoustic and optical modes to the electron-phonon coupling strength in TaC and HfC, we computed the Eliashberg spectral function $\alpha^2F(\omega)$[21] and the corresponding isotropic coupling strength λ (Fig. 3). Consistent with the analysis carried out in relation to Fig. 2, the optical phonons do not play any significant role in the superconducting pairing of TaC ($\lambda_{opt}^{TaC}=0.12$) and HfC ($\lambda_{opt}^{HfC}=0.15$). On the other hand, the acoustic phonons provide an important contribution to the pairing in the case of TaC ($\lambda_{ac}^{TaC}=0.62$), while they remain ineffective in the case of HfC ($\lambda_{ac}^{HfC}=0.09$). Inspection of the Eliashberg function and the phonon density of states (Fig. 3) shows that, in the case of TaC, the spectral weight of $\alpha^2F(\omega)$ is largely enhanced in the acoustic modes, in line with the preceding discussion. The calculated coupling strengths can be used to obtain an estimate of the superconducting transition temperatures of HfC and TaC. For this purpose, we used the McMillan equation with a Coulomb pseudopotential $\mu^\star=0.13$,[25] and obtained $T_c=8.3$ K for TaC and $T_c \lesssim 0.01$ K for HfC, consistent with the experimental values 10.3 and <0.015 K, respectively.[6,11]

The differences in the coupling of Fermi surface electrons

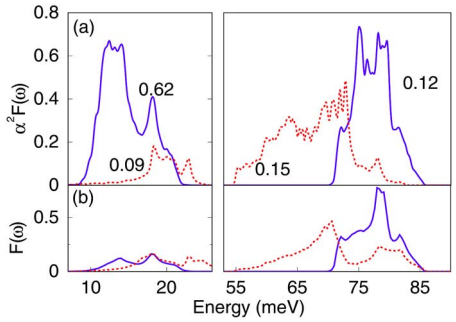

FIG. 3. (Color online) (a) Eliashberg function $\alpha^2F(\omega)$ for TaC (solid) and HfC (dashed). We show the partial contributions to the electron-phonon coupling strength λ next to each curve. (b) The corresponding vibrational density of states $F(\omega)$ in units of modes per meV per unit cell.

to the acoustic and optical phonons in Ta and Hf carbides can be rationalized by inspecting the Wannier-projected electronic density of states [Fig. 4(a)]. The Fermi level of HfC lies near a minimum of the density of states, with partial $2p$ and $5d$ densities of 0.38 and 0.39 states/(eV cell), respectively. The Fermi level of TaC lies 1.35 eV above the corresponding one of HfC, with partial $2p$ and $5d$ densities of 0.24 and 0.78 states/(eV cell), respectively. Surprisingly, while the acoustic coupling in TaC is a factor $\lambda_{ac}^{TaC}/\lambda_{ac}^{HfC} \simeq 6.9$ larger than in HfC, the corresponding ratio between the partial $5d$ density of states is only $0.78/0.39 \simeq 2$. This indicates that the difference in the electron-phonon coupling strengths λ of HfC and TaC cannot be ascribed to a simple density-of-states effect. This observation is supported by the analysis of the nesting function

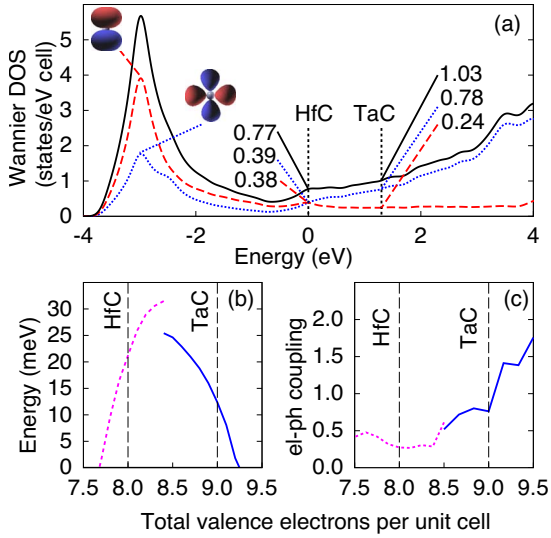

FIG. 4. (Color online) (a) Wannier-projected density of states for TaC and HfC: C-$2p$ (dashed) and metal-$5d$ (dotted) partial density of states, and total density of states (solid). The vertical lines denote the Fermi levels of HfC and TaC. (b) Phonon softening vs doping in HfC (dashed) and TaC (solid): shown is the doping-dependent frequency of the softest mode for each material. (c) Electron-phonon coupling λ as a function of electron concentration for HfC (dashed) and TaC (solid).

[Figs. 1(e) and 1(f)][26] indicating pronounced features arising from the flat parallel sheets of the Fermi surface of TaC, superimposed to the characteristic $1/q$ background.

These results allow us to outline the following picture of the electron-phonon interaction and the superconducting pairing in the transition metal carbides HfC and TaC. (i) The optical modes do not couple significantly to the Fermi surface electrons. This behavior results from the small mass ratio between the carbon and the metal atoms ($m_C/m_{Hf,Ta} \simeq 1/15$, which implies that optical vibrations involve primarily the C atoms), as well as from the small partial density of $2p$ states at the Fermi level. (ii) The acoustic modes mainly couple to the metal $5d$ electrons. This follows from the large $5d$ density of states at the Fermi level, and the fact that acoustic modes involve significant displacements of the metal atoms. (iii) The Fermi surface of TaC offers significant phase space for electron-phonon scattering with large wave vectors, $q \sim 0.7$ (we adopt reciprocal-lattice units throughout). (iv) In the case of HfC, the nesting vectors are considerably smaller in magnitude, $q \lesssim 0.2$, and the associated phase space is negligible. Therefore, while a similar atomistic mechanism operates in both HfC and TaC, the different Fermi surface topology leads to substantially different electron-phonon interaction strengths. These observations indicate that the superconductivity in TaC arises from the coupling of metal d states to acoustic phonons with large wave vectors, and is strongly enhanced by a pronounced Fermi surface nesting. As a consequence, the mechanical hardness of this compound, for which carbon p states play a crucial role,[7] appears to be essentially unrelated to the superconductivity.

The understanding developed so far allows us to discuss directions for optimizing the superconducting transition temperature of superhard carbides. Due to the close connection between the Fermi surface topology and the superconductivity in these compounds, we consider the possibility of optimizing the Fermi surface nesting via substitutional doping. The similarity between the band structures of HfC and TaC suggests that a simple rigid-band model should be suitable for discussing trends. Since a change in the electron concentration will induce a renormalization of the phonon dispersions, we calculated the renormalized vibrational frequencies to identify the stability range of the lattice. Figure 4(b) shows that the addition of 0.32 el/cell to TaC results in a lattice instability driven by a soft longitudinal acoustic (LA) phonon with wave vector $\mathbf{q}=(0.75,0,0)$. On the other hand, a lattice instability associated with a $\mathbf{q}=(0.16,0.50,0.64)$ soft LA mode develops in HfC following the removal of 0.41 el/cell. The instability of electron-doped TaC predicted here is consistent with the fact that stoichiometric group VIb WC is not observed in the cubic structure.[6] Figure 4(a) shows that in order to enhance the contribution of the p states to the electron-phonon coupling, the Fermi level should lie 3 eV below the one of undoped HfC. However, the hole-doping required to produce such a Fermi level shift is well beyond the threshold for the onset of the lattice instability [Fig. 4(b)]. In Fig. 4(c), we show the electron-phonon coupling strength λ recalculated for both HfC and TaC after varying the electron concentration.[27] Within the stability range of the respective lattices, Fig. 4 shows that the

coupling strength of HfC is not very sensitive to the doping, while for TaC it can reach values as high as $\lambda=1.4$ at the onset of the instability. Using this result with the McMillan equation, we find that electron doping of TaC may increase the superconducting transition temperature up to 23 K.

In conclusion, we have shown that the atomistic origin of the superconducting pairing in HfC and TaC resides in the coupling of the transition metal *d* electrons to acoustic phonons. The large difference in the interaction strengths between group IVb HfC and Vb TaC results from the pronounced nesting of the Fermi surface in TaC. Since the other carbides of IVb and Vb transition metals are isoelectronic to HfC and TaC and exhibit similar lattice-dynamical properties, the mechanisms identified in the present work are expected to apply to the entire class of transition metal carbides. More generally, the present study shows that the understanding and design of phonon-mediated superconductors involving light elements and transition metals requires a fine analysis of the delicate interplay between phonon softening, carrier concentration, and Fermi surface topology.

The authors wish to thank M. Coté for many fruitful discussions. Calculations were performed using the QUANTUM-ESPRESSO[28] and WANNIER packages.[29] The Fermi surfaces were rendered with XCRYSDEN.[30] This work was supported by National Science Foundation Grant No. DMR04-39768 and by the Director, Office of Science, Office of Basic Energy Sciences, Division of Materials Sciences and Engineering Division, U.S. Department of Energy under Contract No. DE- AC02-05CH11231. Computational resources have been provided by SDSC and NPACI.

[1] J. Nagamatsu, N. Nakagawa, T. Muranaka, Y. Zenitani, and J. Akimitsu, Nature (London) **410**, 63 (2001).
[2] O. Gunnarsson, Rev. Mod. Phys. **69**, 575 (1997).
[3] S. Yamanaka, K. Hotehama, and H. Kawaji, Nature (London) **392**, 580 (1998).
[4] T. E. Weller, M. Ellerby, S. S. Saxena, R. P. Smith, and N. T. Skipper, Nat. Phys. **1**, 39 (2005).
[5] E. A. Ekimov, V. A. Sidorov, E. D. Bauer, N. N. Mel'nik, N. J. Curro, J. D. Thompson, and S. M. Stishov, Nature (London) **428**, 542 (2004).
[6] L. E. Toth, *Transition Metal Carbides and Nitrides* (Academic, New York, 1971).
[7] S.-H. Jhi, J. Ihm, S.G. Louie, and M.L. Cohen, Nature (London) **399**, 132 (1999).
[8] A. Y. Liu, R. M. Wentzcovitch, and M. L. Cohen, Phys. Rev. B **38**, 9483 (1988).
[9] W. Hanke, J. Hafner, and H. Bilz, Phys. Rev. Lett. **37**, 1560 (1976).
[10] W. Weber, Phys. Rev. B **8**, 5082 (1973).
[11] P. B. Allen and M. L. Cohen, Phys. Rev. Lett. **29**, 1593 (1972).
[12] E. I. Isaev, R. Ahuja, S. I. Simak, A. I. Lichtenstein, Y. K. Vekilov, B. Johansson, and I. A. Abrikosov, Phys. Rev. B **72**, 064515 (2005).
[13] H. R. Zeller, Phys. Rev. B **5**, 1813 (1972).
[14] B. Klein, L. Boyer, and D. Papaconstantopoulos, Solid State Commun. **20**, 937 (1976).
[15] B. Klein and D. A. Papaconstantopoulos, Phys. Rev. Lett. **32** 1193 (1974).
[16] F. Giustino, M. L. Cohen, and S. G. Louie, Phys. Rev. B **76**, 165108 (2007).
[17] F. Giustino, J. R. Yates, I. Souza, M. L. Cohen, and G. Louie, Phys. Rev. Lett. **98**, 047005 (2007).
[18] D. M. Ceperley and B. J. Alder, Phys. Rev. Lett. **45**, 566 (1980).
[19] Valence electronic wave functions were expanded in a plane-wave basis with an energy cutoff of 90 Ry [J. Ihm, A. Zunger, and M. L. Cohen, J. Phys. C **12**, 4409 (1979)], and the core-valence interaction was taken into account through norm-conserving pseudopotentials [N. Troullier and J. L. Martins, Phys. Rev. B **43**, 1993 (1991); M. Fuchs and M. Scheffler, Comput. Phys. Commun. **119**, 67 (1999)].
[20] S. Baroni, S. de Gironcoli, A. Dal Corso, and P. Giannozzi, Rev. Mod. Phys. **73**, 515 (2001).
[21] P. B. Allen and B. Mikovic, in *Solid State Physics*, edited by H. Ehrenreich, F. Seitz, and D. Turnbull (Academic, New York, 1982), Vol. 32, p. 1.
[22] N. Marzari and D. Vanderbilt, Phys. Rev. B **56**, 12 847 (1997); I. Souza, N. Marzari, and D. Vanderbilt, *ibid.* **65**, 035109 (2001).
[23] H. G. Smith and W. Gläser, Phys. Rev. Lett. **25**, 1611 (1970); *Proceedings of the International Conference on Phonons, Rennes, France, 1971*, edited by M. A. Nusimovici (Flammarion, Paris, 1972).
[24] L. Pintschovius and B. Scheerer, J. Phys. C **11**, 1557 (1978).
[25] G. Grimvall, *The Electron-Phonon Interaction in Metals* (North-Holland, Amsterdam, 1981).
[26] M. Gupta and A. J. Freeman, Phys. Rev. B **14**, 5205 (1976).
[27] We calculated the renormalization of the vibrational frequencies using the real part of the phonon self-energy in the Migdal approximation.[17]
[28] S. Baroni, A. Dal Corso, S. de Gironcoli, P. Giannozzi, C. Cavazzoni, G. Ballabio, S. Scandolo, G. Chiarotti, P. Focher, A. Pasquarello, K. Laasonen, A. Trave, R. Car, N. Marzari, and A. Kokalj, http://www.pwscf.org.
[29] A. A. Mostofi, J. R. Yates, Y.-S. Lee, I. Souza, D. Vanderbilt, and N. Marzari, Comput. Phys. Commun. **178**, 685 (2008).
[30] A. A. Kokalj, J. Mol. Graphics Modell. **17**, 176 (1999).